Suplemmentary Materials

Ionogels Derived from Fluorinated Ionic Liquids to Enhance Aqueous Drug Solubility for Local Drug Administration

Carolina Hermida-Merino [1], David Cabaleiro [1], Carlos Gracia-Fernández [2], Jesus Valcarcel [3], José Antonio Vázquez [3], Noelia Sanz [4], Martín Pérez-Rodríguez [1], Maria Arenas-Moreira [5], Dipanjan Banerjee [6,7], Alessandro Longo [8,9], Carmen Moya-Lopez [10], Luis Lugo [1], Patrice Bourson [10], Ana B. Pereiro [11], Georges Salloum-Abou-Jaoude [12], Iván Bravo [5], Manuel M. Piñeiro [1,*] and Daniel Hermida-Merino [1,6,*]

Table S1. pHs of the IL and IL/H_2O emulsions.

Samples	pH	T (°C)
H_2O	6.23	27.4°C
1IL/H_2O	7.44	28.5°C
5IL/H_2O	7.45	28.6°C
10IL/H_2O	7.49	29.1°C
15IL/H_2O	7.51	29.1°C
25IL/H_2O	7.51	29.1°C
IL	6.67	27.9°C

Table S2. Summary of the fitting of the IL/Water emulsions SAXS profiles to adjusted to the weakly correlated nanoscale mass fractal aggregates model with a radius of gyration Rg associated with the fractal size and the fractal dimension D that define their compactness and Ionogels and ξ being the correlation length. The 1IL/Water was not fitted due to the lack of structure and therof the fitting parameters are filled in the table as not applicable (NA).

	1IL/Water	5IL/Water	10IL/Water	15IL/Water	25IL/Water
R_g	NA	1.73	1.72	1.68	1.55
ξ	NA	2.99	2.82	2.5	2.34
D_f	NA	3.28	3.55	4	4

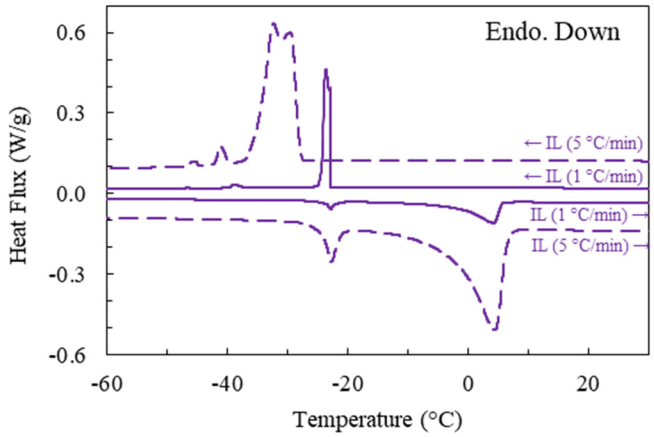

Figure S1. DSC thermogram of the cooling and heating cycles obtained for [C_2C_1py][$C_4F_9SO_3$] ionic liquid at 1 °C/min and 5 °C/min.

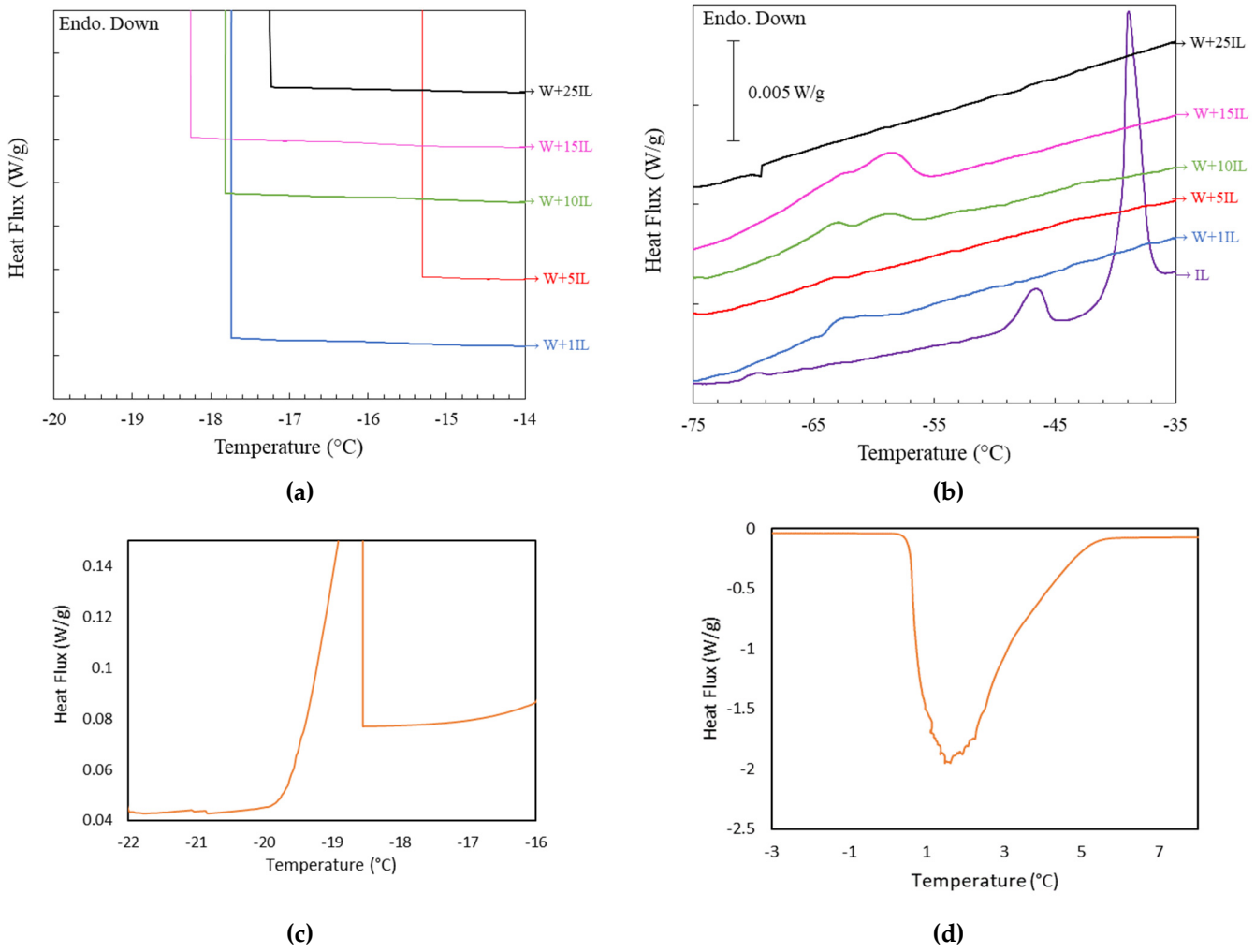

Figure S2. DSC thermogram (**a**, **b**) Cooling ramp of (—) Water, (—) 1IL/Water, (—) 5IL/Water, (—) 10IL/Water, (—) 15IL/Water, (—) 25IL/Water and (—) IL at 1 °C/min; (c) Cooling ramp of (—) Water at 1 °C/min; (d) Heating ramp of (—) Water at 1 °C/min.

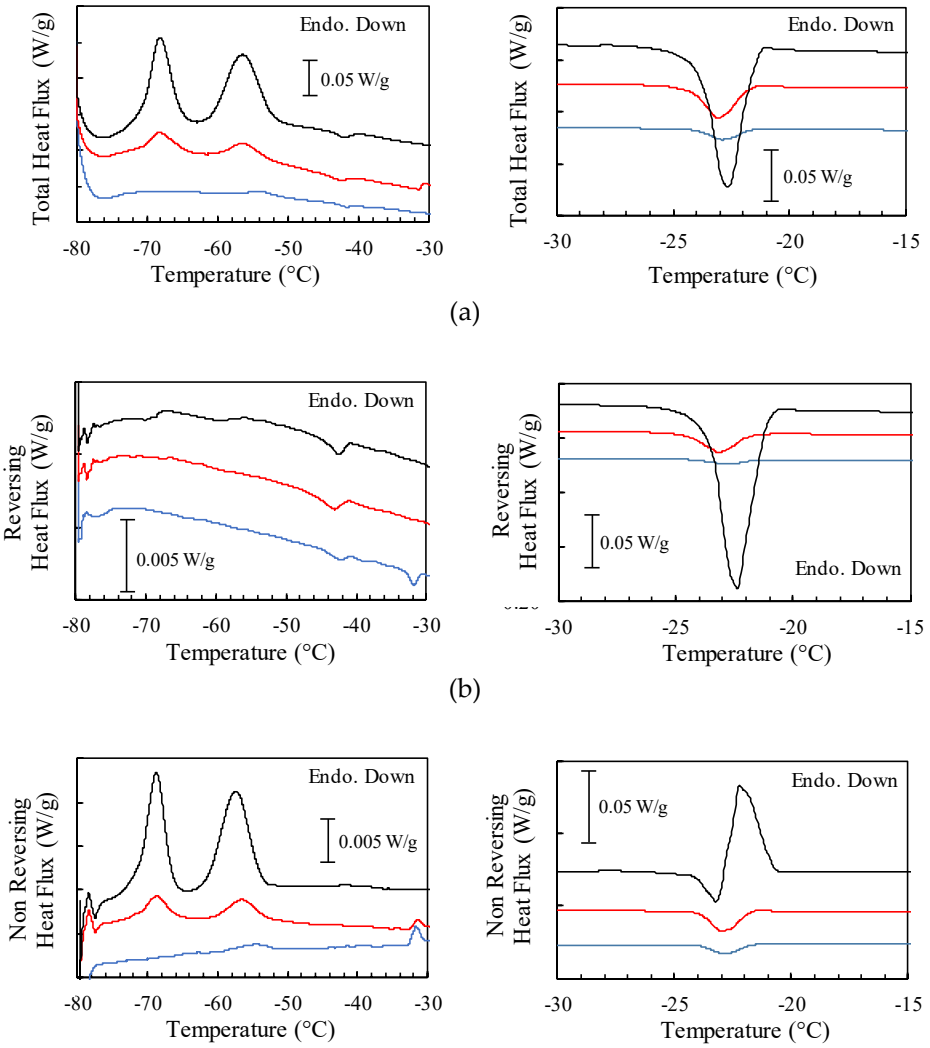

Figure S3. (**a**) Total; (**b**) reversing and; (**c**) non-reversing heat fluxes from heating MDSC runs at 1 °C/min for some representative IL/water emulsions: (—) 1IL/Water, (—) 5IL/Water, and (—) 25IL/Water.

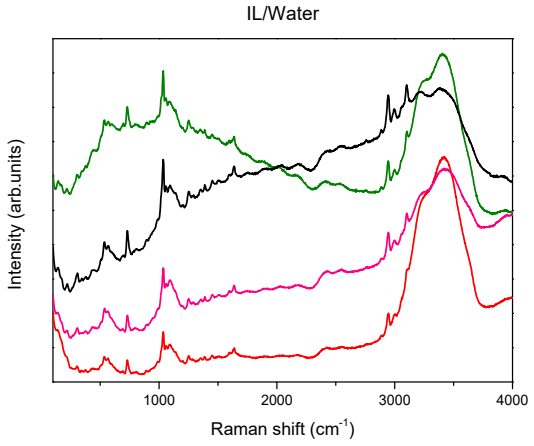

Figure S4. Raman spectra of (—) 5IL/Water, (—) 10IL/Water, (—) 15IL/Water, (—) 25IL/Water.

Table S3. Summary of the fitting of the 25IL/Water emulsion loaded with DOX SAXS profiles to adjusted to the weakly correlated nanoscale mass fractal aggregates model with a radius of gyration Rg associated with the fractal size and the fractal dimension D that define their compactness and Ionogels and ξ being the correlation length.

	25IL/Water/ DOX_1mg/ml	25IL/Water/ DOX_2mg/ml	25IL/Water/ DOX_5mg/ml	25IL/Water/ DOX_10mg/ml
R_g	1.64	1.66	1.78	1.07
ξ	2.31	2.3	2.36	1.63
D_f	4.00	3.96	3.75	3.8

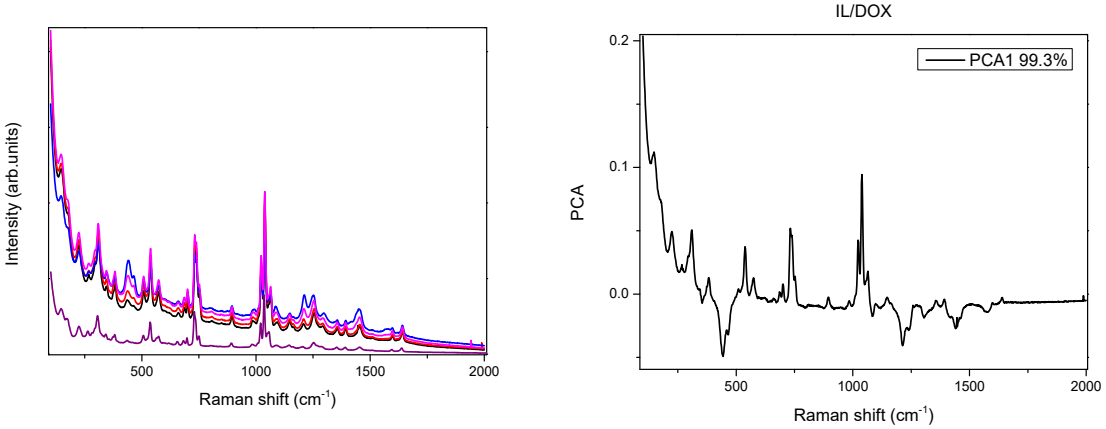

Figure S5. Raman spectra of: (**a**) 25IL/Water loaded with DOX; (**b**) and the corresponding PCA.

Table S4. Main FTIR vibration bands associated with IL and gelatin nanostructure.

Functional group	GE	GE/1IL	GE/5IL	GE/10IL	GE/15IL	GE/25IL	IL
	Wavenumber (cm^{-1})						
N-H , O-H	**3321**	**3334**	**3272**	**3353**	**3353, 3300**	3353, 3300	---
Aliphatic tension CH	2850-3000	2850-3000	2850-3000	2850-3000	2850-3000	2850-3000	2951, 3000
Aromatic CH tension	---	---	---	---	---	---	3067
Aliphatic CH flexion	1337, 1458	1388, 1458	1384, 1457	1381, 1457	1338, 1457	1338, 1457	1390, 1459
Amide I,II,III	1633, 1553, 1250	1634, 1553, 1250	1635, 1552, 1250	1637, 1552, 1251	1637, 1551, 1251	1637, 1550, 1251	---
Tension C-O,C-O-C carbohydrates	1163, 1082	1163, 1082, 1064	1137,1082 , 1062	---	---	---	---
Water	600	600	600	600	600	600	---
C-F (CF_2 group)	---	---	1130-1290	---	1137-1290	1137-1290	1207-1253, 1131

C=C (pyridinium ring)	---	---	---	---	---	---	1638-1600
C=N (pyridinium ring)	---	---	---	---	---	---	1508, 1459
Pyridinium ring strain	---	---	1000	1000	1007	1000	1006
S-O stress mode (SO_3 group)	---	---	1020, 1060	1000, 1061	1000, 1060	1000, 1060	1055, 1048, 1020
S-O bending mode (SO_3 group)	---	---	600-700	600-700	600-700	600-700	600-700
S=O bond (SO_3 group)	---	---	1350	1352	1352	1352	1352
Flexion O=S=O	---	---	---	---	525	525	522-530

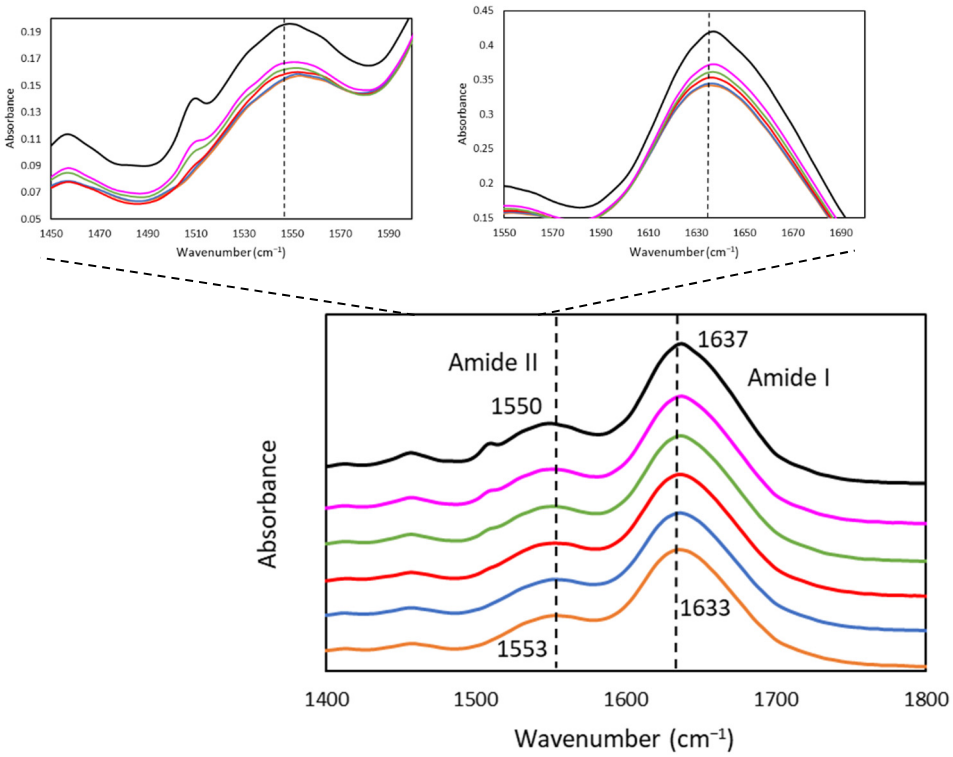

Figure S6. FTIR Spectra of Amide I and Amide II for: (—) GE, (—) GE/1IL, (—) GE/5IL, (—) GE/10IL, (—) GE/15IL and (—) GE/25IL.

Table S5. FTIR bands of Amide I and Amide II for: GE, GE/1IL, GE/5IL, GE/10IL, GE/15IL and GE/25IL.

Samples	Amide I (cm^{-1})	Amide II (cm^{-1})
GE	1633	1553
GE/1IL	1634	1553
GE/5IL	1635	1552
GE/10IL	1637	1552
GE/15IL	1637	1551
GE/25IL	1637	1550

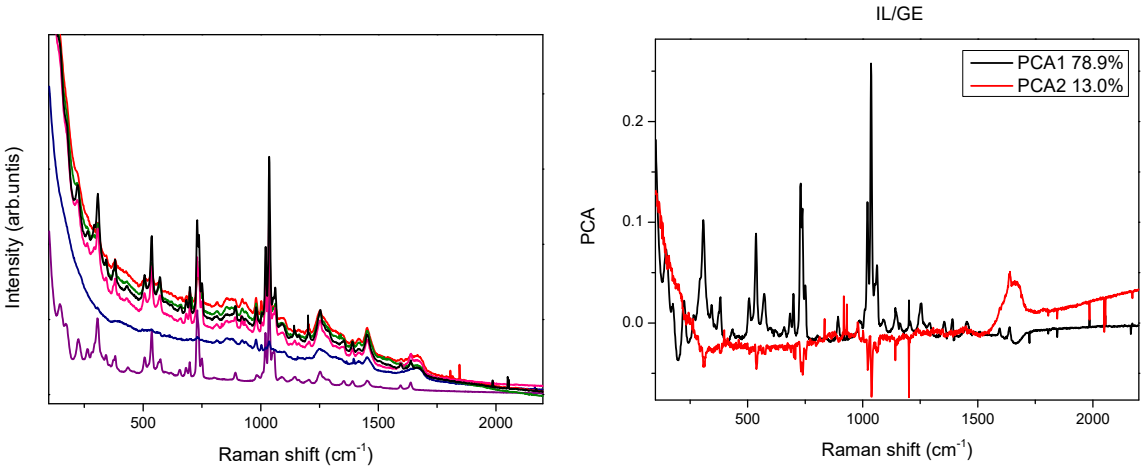

(a) **(b)**

Figure S7. (**a**) Raman spectra of the Ionogels and; (**b**) their corresponding PC1 an PC2.

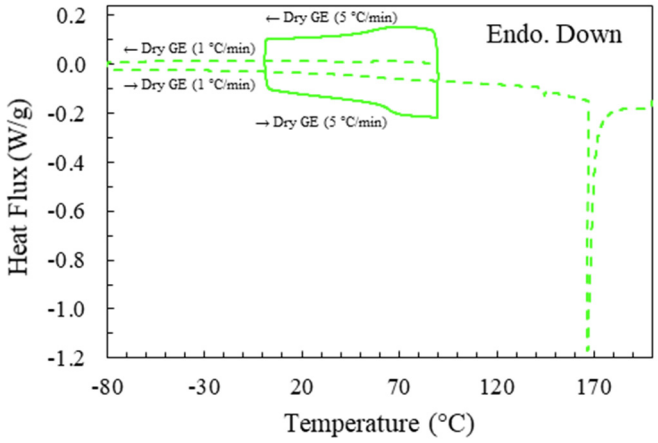

Figure S8. DSC cooling and heating thermograms obtained for dry shark gelatin.

Table S6. Enthalpies and Temperature of crystallization of water in the different hydrogel and Ionogels.

	GE	IL	W	T (ºC)	Δh (J/g)
GE	25	0	75	-0.29	178.3
GE+1IL	25	1	74	- 1.25	152.6
GE+5IL	25	5	70	-1.09	149.3
GE+10IL	25	10	65	-1.10	164.4
GE+15IL	25	15	60	-1.43	135.6
GE+25IL	25	25	50	-2.04	110.2
Water	0	0	100	1.47	308.7

Table S7. Summary of the fitting of the SAXS profiles to a a heterogeneous sphere with fractal structure with with a radius of gyration Rg associated with the fractal size and the fractal dimension D that define their compactness and Ionogels and ξ being the correlation length.

	Ge/1IL 10°C	Ge/1IL 25°C	Ge/5IL 10°C	Ge/5IL 25°C	Ge/10IL 10°C	Ge/10IL 25°C	Ge/15IL 10°C	Ge/15IL 25°C	Ge/25IL 0°C	Ge/25IL 25°C
R_g	0.89	0.92	1.00	1.06	1.00	1.08	1,00	1.06	1.01	0.98
ξ	1.22	2.13	1.68	2.46	1.99	1.92	2.13	1.62	1.28	1.14
D_f	3.27	2.63	3.0	2.6	2.92	2.93	2.53	2.9	3.84	3.22

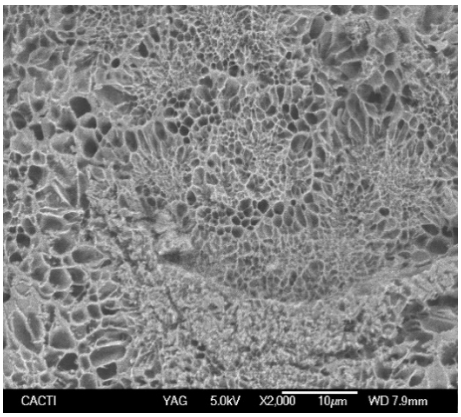

(**a**)

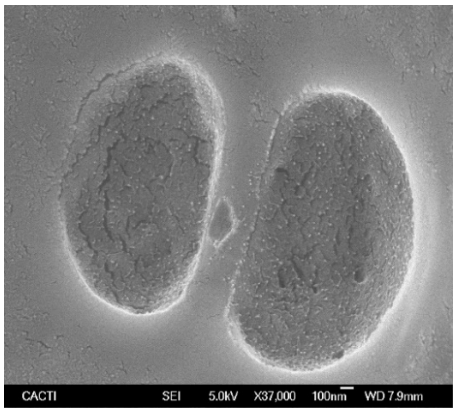

(**b**)

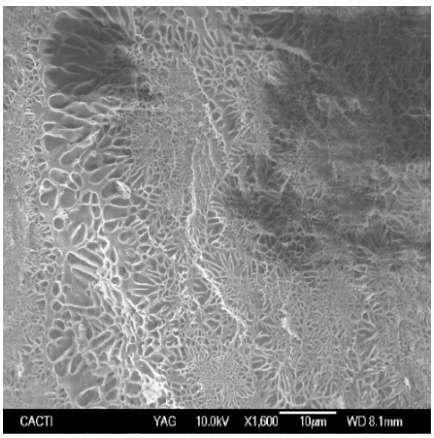

(**c**)

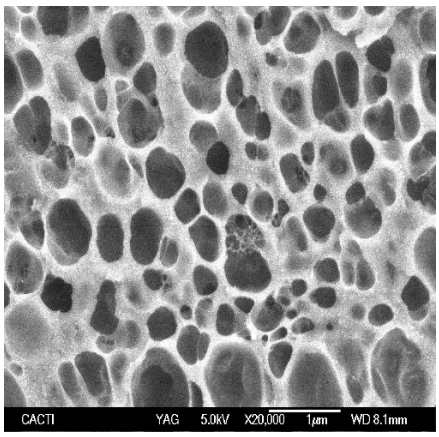

(**d**)

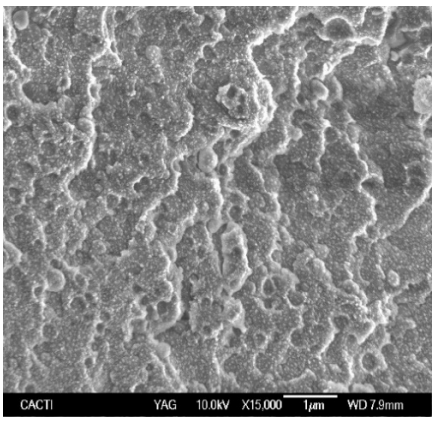

(e)

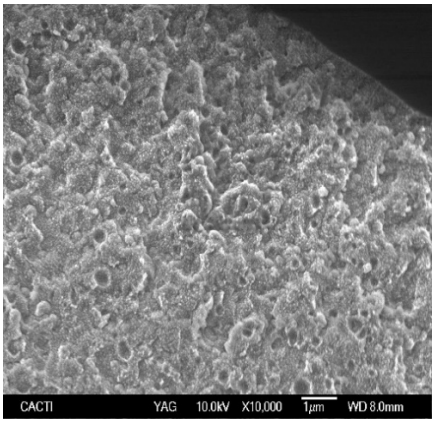

(f)

Figure S9. Cryo-scanning electron microscopy of: (**a**, **b**) Shark gelatin hydrogel, (**a**) X2000; (**b**) X37000; (**c**) GE/5IL at X1600; (**d**) GE/15IL at X20000; (**e**) and (**f**) GE/25IL at X15000.

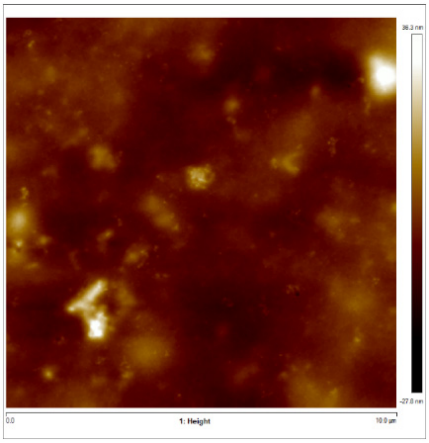

(a)

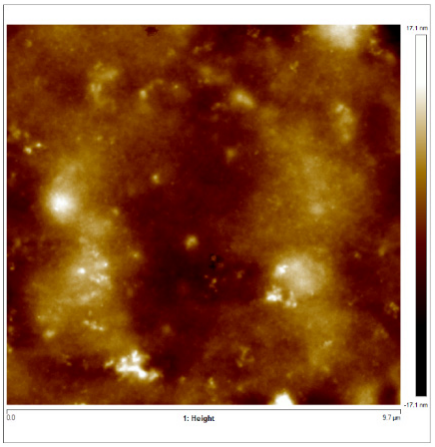

(b)

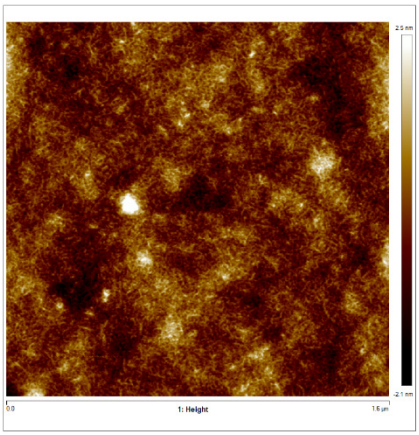

(c)

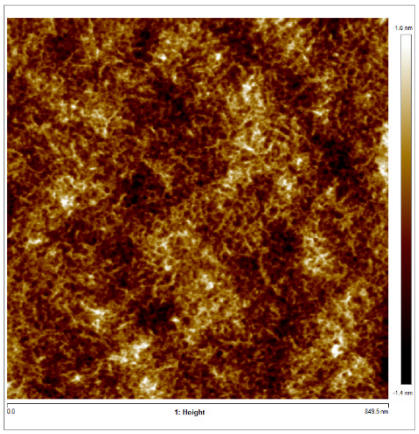

(d)

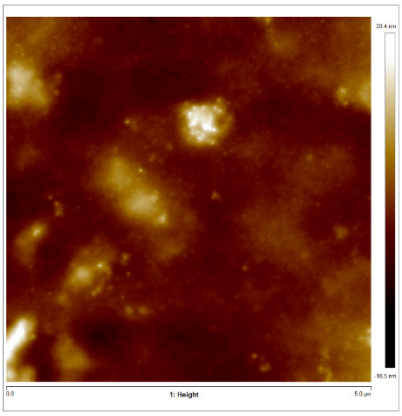

(e)

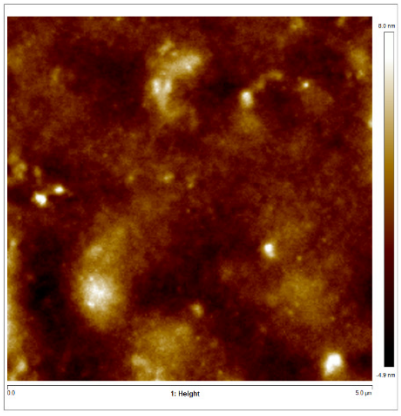

(f)

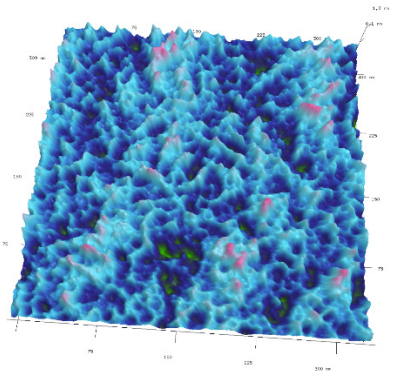

(g)

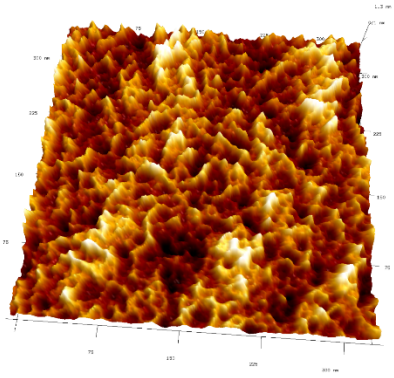

(h)

Figure S10. FM images of shark gelatin hydrogel. (**a**) Zone 1 at a magnification of 10x10 μm², (**b**) Zone 2 at a magnification of 10x10 μm². (**c**) Image 2D with a field of view 1.6X1.6 μm², (**d**) Image 2D with a field of view 849.5X849.5 μm², (**e**) Image 2D in Zone 1 at a magnification of 5x5 μm², (**f**) Zone 2 at a magnification of 5x5 μm²; (**g**), (**h**) Zone 1, Image 3D.

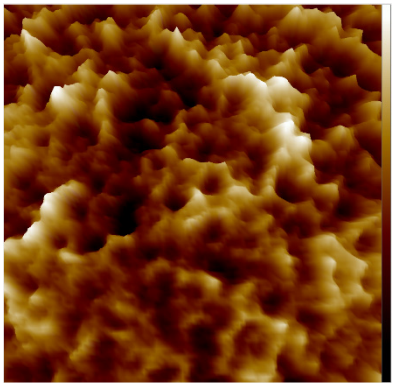

(**a**)

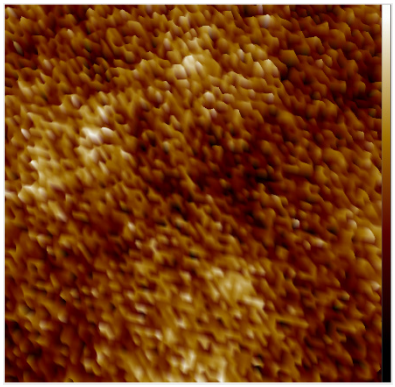

(**b**)

Figure S11. Zoom images 3D with magnifications 120x120 nm² of shark gelatin hydrogel. (**a**) Zone 1; (**b**) Zone 2.

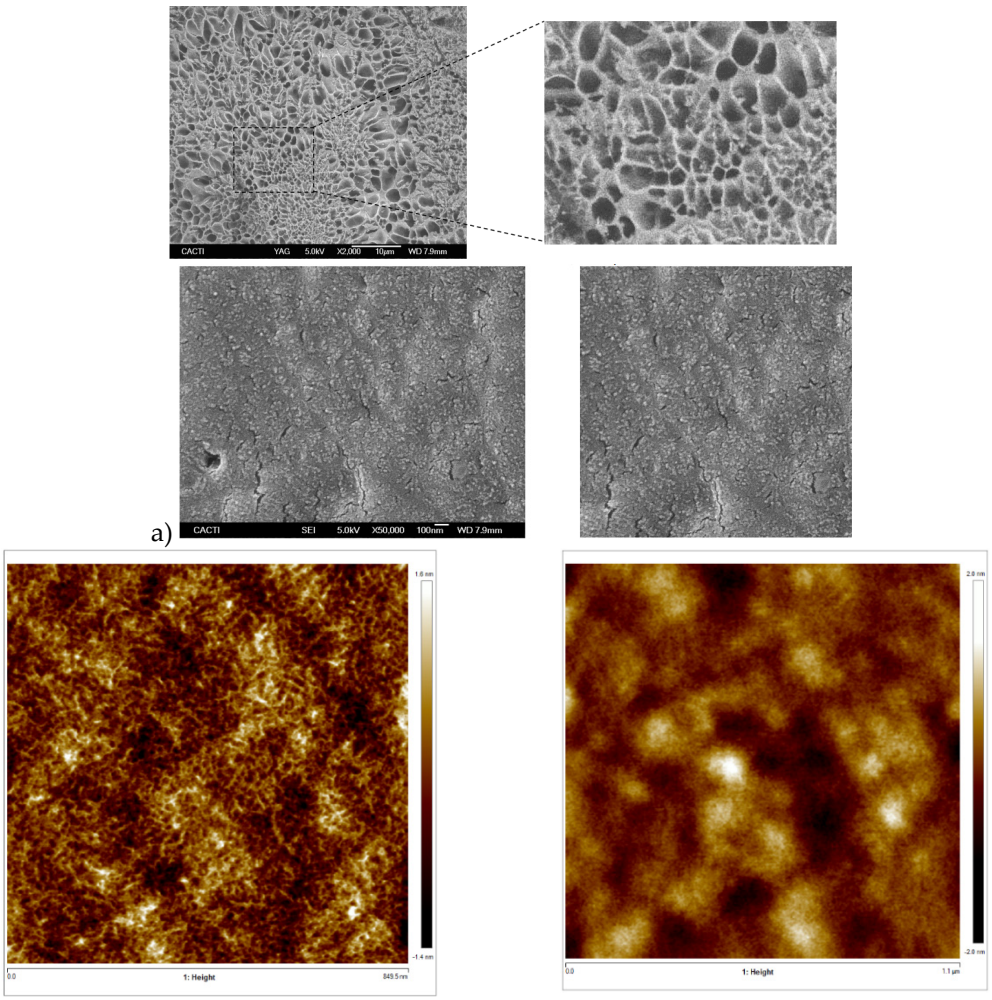

Figure S12. (**a**) Cryo-SEM images; (**b)** Image of Zone 1 at a magnification of 0.84X0.84 μm^2; (**c**) Image of Zone 2 at a magnification of 1.1X1.1 μm^2 of hydrogel gelatin.

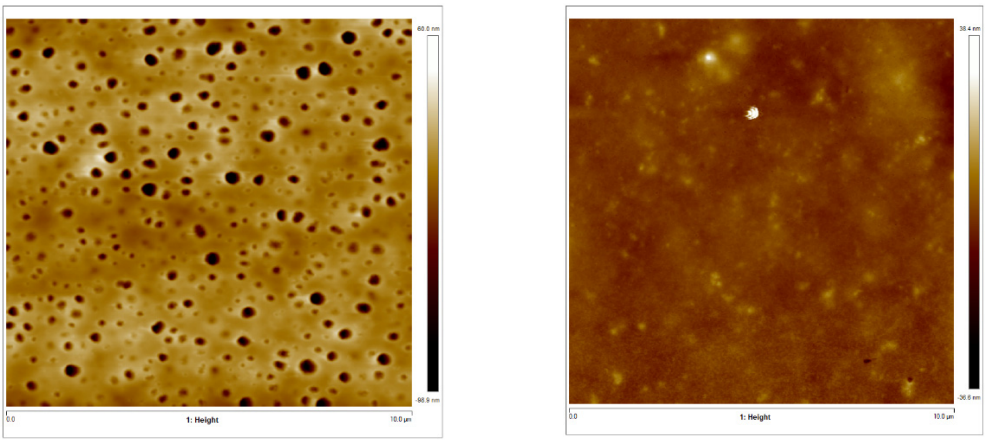

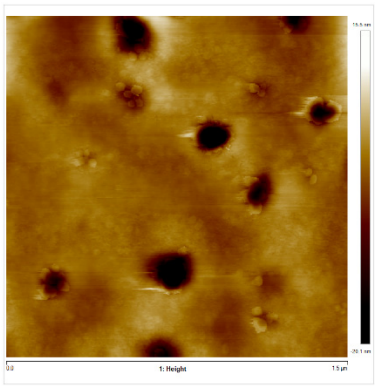

(c)

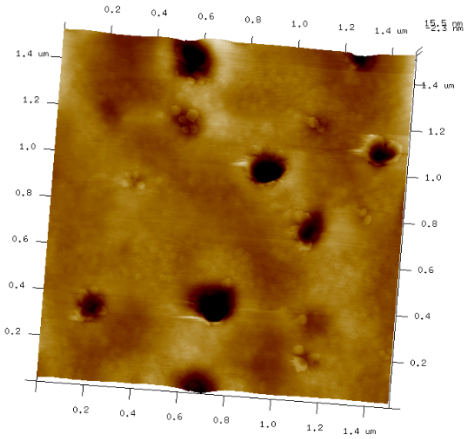

(d)

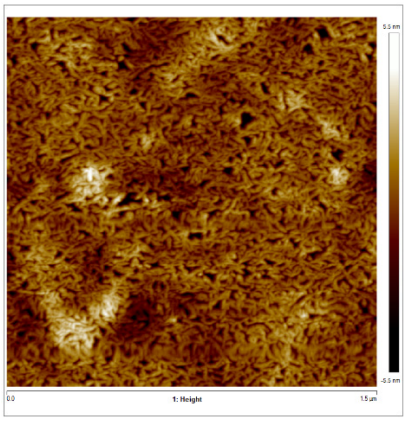

(e)

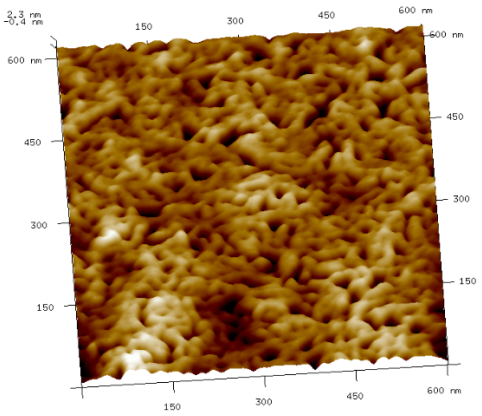

(f)

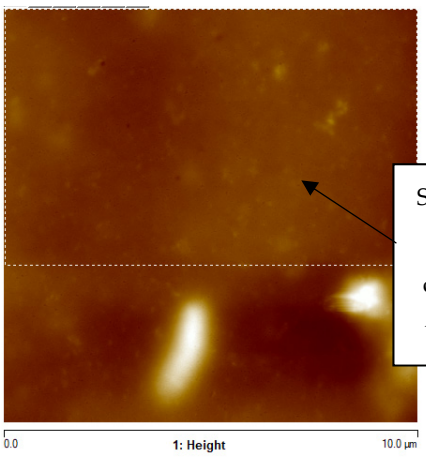

(g)

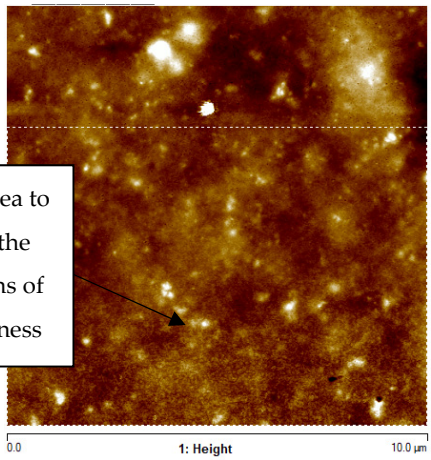

(h)

Figure S13. (**a**) Zone 2 of GE/25IL; (**b**) Zone 2 of GE/5IL Topographic 2D images Zone 2, 10x10 µm²; (**c**) Zone 1, Image 2D Field of View 1.5X1.5 µm² of GE/25IL; (**d**) Zone 1, Image 3D Field of View 1.5X1.5 µm² of GE/25IL; (**e**) Zone 1, Image 2D, Field of View 1.5X1.5 µm² of GE/5IL; (**f**) Zone 1, Image 3D Field of View 1.5X1.5 µm² of GE/25IL; (**g**) GE/5IL of Zone 1; (**h**) GE/5IL of Zone 2.

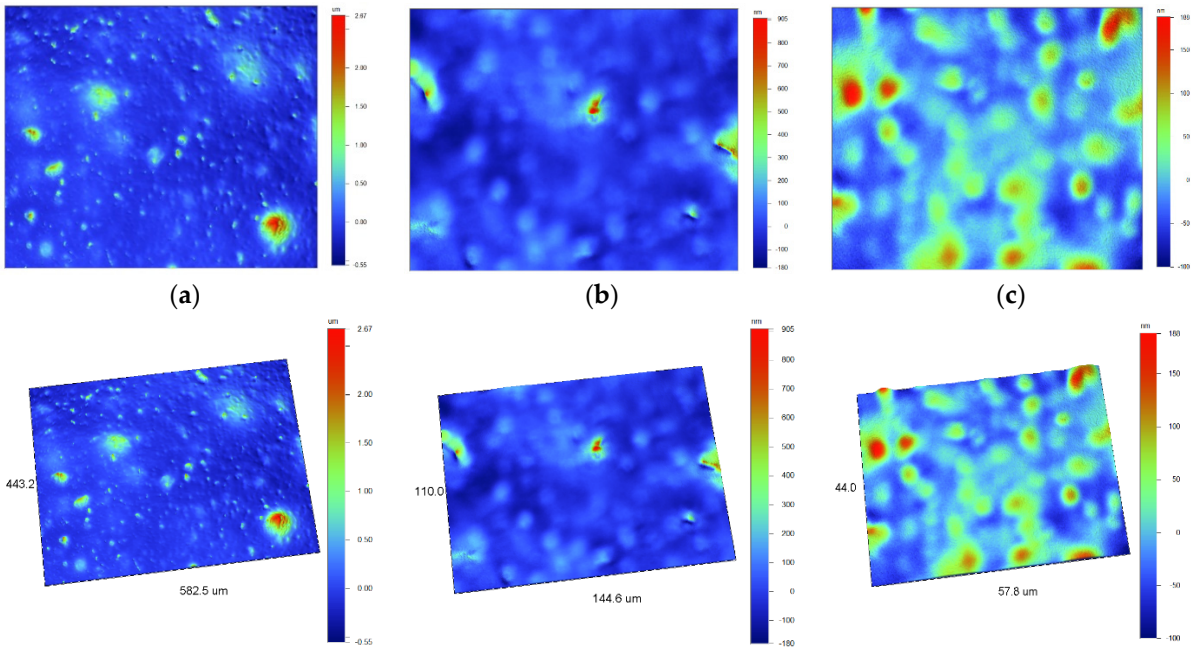

Figure S14. Imaging of WLOP method. (**a**) 2D image at 5x_2x (443.2X582.5 μm²; (**b**) 20x_2x (110X144 μm²; (**c**) 250x_2x (44X58 μm²); (**d**) 3D magnification 5X_FOV 2X (443.2X582.5 μm²; (**e**) 3D magnification 20X_2X (110X144μm²), (**f**) 3D magnification 50X_2X (44X58μm²).

The development of the calculations of the three-dimensional roughness parameters (Sa, Sq, Sz, Ssk and Sku), have been developed in previous studies [1].

Table S8. Roughness parameter values obtained by WLOP of shark gelatin hydrogel.

INTERFEROMETRIC OPTICAL PROFILOMETRY / 3D Amplitude Roughness Parameters					
	Sa (nm)	**Sq (nm)**	**Sz (nm)**	**Ssk**	**Sku**
5X_2X	148.07	241.84	2160.00	3.53	22.76
20X_2X	54.31	80.55	780.03	2.53	16.66
50X_2X	27.73	37.31	251.27	1.14	5.12

The gelation point of the Ionogles was determined by monitoring the loss and storage moduli, as well as the complex viscosity (Figure S15). A transition in the complex viscosity occurs in the thermal range between 15 °C and 22 °C as well as in the storage and loss moduli during the heating ramp, which is indicative of the interruption of the elastic network of the hydrogel and of in agreement with the sol/gel transition observed for the gelatin hydrogel and which is slightly lower for the Ionogels.

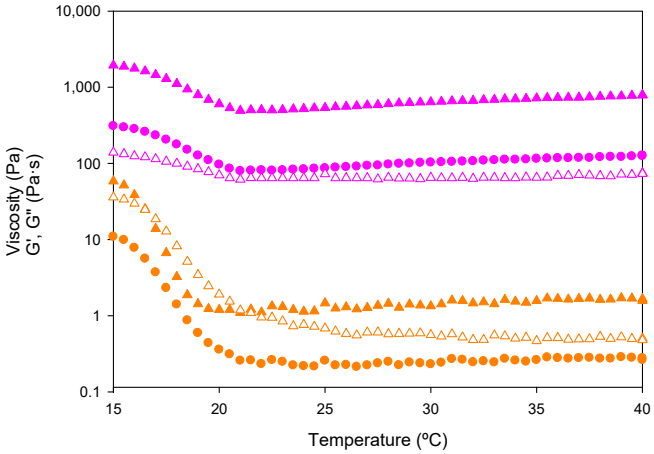

Figure S15. Complex viscosity variation (filled ○); and storage modulus (G', filled Δ) and loss modulus (G'', open Δ) versus temperature of gelatin hydrogel (orange color) and Ionogel (fuchsia color).